

# First Identification of the Effects of Low Frequency Electromagnetic Field on the Micromolecular Changes in Adipose Tissue-Derived Mesenchymal Stem Cells by Fourier Transform Infrared Spectroscopy

Kornelia Łach, Józef Cebulski<sup>1</sup>, Radosław Chaber, Beata Kocan<sup>2</sup>, Renata Wojnarowska-Nowak<sup>3</sup>, Agnieszka Banaś-Ząbczyk<sup>4</sup>

Department of Pediatrics, Institute of Medical Sciences, Medical College of Rzeszow University, University of Rzeszow, Warzywna 1A, <sup>1</sup>Institute of Physics, College of Natural Sciences, <sup>3</sup>Institute of Material Engineering, College of Natural Sciences, University of Rzeszow, Pigońia 1, <sup>2</sup>Centre for Innovative Research in Medical and Natural Sciences, Medical College of Rzeszow University, University of Rzeszow, Warzywna 1A, 35-310 Rzeszow, <sup>4</sup>Department of Biology, Institute of Medical Sciences, Medical College of Rzeszow University, Al. Mjr. W. Kopisto 2a, 35-959 Rzeszow, Poland

## Abstract

**Purpose:** In this study, we hypothesize that exposure of adipose tissue-mesenchymal stem cells (AT-MSCs) to electromagnetic field (EMF) may impact adipose stem cells' micromolecular structure (analyzed using Fourier transform infrared spectroscopy [FTIR]). **Materials and Methods:** The AT-MSCs were exposed to continuous vertically applied sinusoidal EMF with a frequency of 50 Hz and a flux density of 1.5 mT for 24, 48, and 72 h. After an appropriate time (24, 48, 72 h) cells were washed with PBS, scrubbed, and immediately taken into FTIR analyses. **Results:** EMFs affect AT-MSCs. The greatest differences were in the range of nucleic acids and proteins in the fingerprint region which occurred after 24 and 48 h of EMF exposure. However, in the case of 72 h of EMF exposure, no significant differences were noticed in the FTIR spectra towards the control. **Conclusions:** FTIR spectra show differences between samples under the influence of EMF before they will be manifested at the morphological level. The largest differences in the range of nucleic acids and proteins in the fingerprint region occurred at 24 and 48 h of EMF exposure. That means it was during the first 48 h after EMF exposure a great number of dynamic changes occurred. However, in the case of AT-MSCs in 72 h EMF and 72 h control, no significant differences were noted in the FTIR spectra, which means that the chemical composition in these two cases is similar. EMF is not neutral for stem cells, especially in the in the first hours of interaction (24 h, 48 h).

**Keywords:** Adipose tissue-mesenchymal stem cells, electromagnetic field, fourier transform infrared spectroscopy, human adipose tissue-derived mesenchymal stem cells, mesenchymal stem cell

Received on: 20-04-2021

Review completed on: 09-07-2021

Accepted on: 10-07-2021

Published on: 20-11-2021

## INTRODUCTION

Adult stem cells are undifferentiated cells with high renewable capacity that can differentiate into many other cell types. Currently, interest in mesenchymal stem cells (MSC) from adipose tissue (AT-MSCs), (so-called adipose stem/stromal cells (ASCs), adipose-derived stromal cells (ADSCs); adipose stromal cells (ASC); adipose MSCs (AdMSCs); AT-derived MSCs (AT-MSCs); lipoblasts; pericytes; preadipocytes; processed lipoaspirate cells) is increasing due to their abundance and high availability without ethical concerns.<sup>[1-3]</sup> Adult stem cells, including mesenchymal stem cells participate in regenerative processes, wound healing,

immunomodulation, and in particular they reveal high trophic activity.<sup>[4,5]</sup>

Even though electromagnetic fields (EMF) is existing naturally all over since ever, in the last few decades the human-made EMF has been invading the human environment. Nowadays,

**Address for correspondence:** Mrs. Kornelia Łach, Department of Pediatrics, Institute of Medical Sciences, Medical College, University of Rzeszow, Warzywna 1A, 35-310 Rzeszow, Poland. E-mail: kornelia\_łach@wp.pl, kolach@ur.edu.pl

This is an open access journal, and articles are distributed under the terms of the Creative Commons Attribution-NonCommercial-ShareAlike 4.0 License, which allows others to remix, tweak, and build upon the work non-commercially, as long as appropriate credit is given and the new creations are licensed under the identical terms.

**For reprints contact:** WKHLRPMedknow\_reprints@wolterskluwer.com

**How to cite this article:** Łach K, Cebulski J, Chaber R, Kocan B, Wojnarowska-Nowak R, Banaś-Ząbczyk A. First identification of the effects of low frequency electromagnetic field on the micromolecular changes in adipose tissue-derived mesenchymal stem cells by fourier transform infrared spectroscopy. J Med Phys 2021;46:253-62.

### Access this article online

Quick Response Code:



Website:  
www.jmp.org.in

DOI:  
10.4103/jmp.jmp\_57\_21

we do not have a well-established knowledge about its biological impact. However, there are reports in the literature claiming that long-term exposure to certain EMFs is a risk factor for diseases such as Alzheimer's disease, some cancers, and male infertility.<sup>[6,7]</sup> The WHO/International Agency for Research on Cancer classified extremely low-frequency EMFs as "a possibly carcinogenic to humans," based on an increased risk for childhood leukemia and for malignant glioma (type of brain cancer).<sup>[8]</sup>

On the other hand, the EMF is used in medicine, as a safe, noninvasive method for treatment or diagnostic purposes. It is successfully adapted in physiotherapy for the treatment of osteoarthritis or bone disorders as well as for cartilage regeneration or pain reduction.<sup>[9]</sup> The nonionizing EMF has also found its application to brain cancer treatment in the case when the tumor is inoperable.<sup>[10]</sup>

We suppose, that there is a certain hierarchy at biological levels on which the subsequent effects occur—first, at the molecular level, then at the cellular level, and finally at the functional level. The ease of early detection of changes depends strictly on the level at which they appear. The changes at the molecular level take place at the very beginning, often at nanoscale ranges and therefore, they are the most difficult to capture. On the other hand, revealing of these very early effects is of high significance, because it gives us information that changes on subsequent levels will be implemented. At present, these processes are monitored *via* the use of a variety of molecular biological methods, such as *in vitro* and *in vivo* assays, flow cytometry, real-time polymerase chain reaction (RT-PCR) or microarray technologies.<sup>[11]</sup> However, many of these routinely used techniques are time-consuming (staining) and drying steps that destroy cellular characteristics.<sup>[4]</sup> So there is a need for nondestructive methods which can provide, in a reproducible manner, reliable information about natural processes within living stem cells. In this perspective, the vibrational spectroscopic techniques seem to be a proper tool for investigation on stem cells biology. Fourier transforms infrared (FTIR) spectroscopy method, which enable to gain a direct information about the biochemical composition on the molecular level. This technique does not require additional reagents/kits, is relatively simple, reproducible, nondestructive, and only small amounts of material with a minimum sample preparation are required.<sup>[12]</sup>

It can be clearly concluded from the studies in the literature that FTIR spectroscopy is a formidable technique used to obtain the molecular fingerprint in a tested sample, which absorbs the IR wave according to the chemical and structural bonds of molecules in biological samples. It can provide information about the structure of biomolecules such as lipids, proteins, carbohydrates, and nucleic acids, giving rise to a series of identifiable functional groups' bands.<sup>[12,13]</sup> Obtained specific spectral bands are relatively narrow, easy to analyze and sensitive to molecular structure, conformation, and environment.<sup>[14-16]</sup> One of the main difficulties of using

FTIR spectroscopy for biological applications in fluid is the presence of water. Water has a strong absorption over a broad range and it can mask the absorption of the rest components of the examined tissue. This is why, many researchers decide to test liquids in dry form, which greatly affects the appearance of the spectrum but this is no longer a study on live cells in their natural aqueous state.<sup>[17-22]</sup> The best way to get rid of this problem is to use FTIR spectrometers with an Attenuated Total Reflection (ATR) element. This technique allows on the measurements of IR absorption spectra in solution.<sup>[23-25]</sup>

Many researchers try to identify mechanisms based on molecular or cellular changes that are brought about by the EMF—this would provide people to know how physical forces might be converted into a biological action.<sup>[26-28]</sup> FTIR spectroscopy should allow testing of our hypothesis that the EMF influences and directs the stem cells towards the different programs (such as differentiation, death, neoplastic transformation, etc.), depending on the EMF dose (EMF frequency, magnetic induction, shape of signal, and time of the treatment, continuous or intervals), each of them having great influence on very sensitive biological systems within adipose tissue-derived mesenchymal stem cells.<sup>[29]</sup>

The purpose of this study was the attempt to use FTIR spectroscopy in studies of the effects of low-frequency EMF on the micromolecular changes in adipose tissue-derived mesenchymal stem cells.

For this purpose, measurements in the range of 800–3500  $\text{cm}^{-1}$ , using FTIR spectroscopy were used and the following analyzes were performed:

- Comparison of EMF exposed and nonexposed stem cells' spectroscopic spectra. Presented data represent changes in the structure of proteins, lipids, and nucleic acids between samples (AT-MSC in three different EMF continuous exposure durations: 24 h, 48 h, 72 h and AT-MSC control: 24 h, 48 h, 72 h (without EMF exposure))
- Performing of principal component analysis (PCA) analysis of the obtained spectra.

## MATERIALS AND METHODS

### Adipose tissue-mesenchymal stem cells culturing

Commercially available StemPRO® Human Adipose-Derived Stem Cells, lot no 1001001, Invitrogen™) were cultured in reduced serum (2%), human mesenchymal stem cell growth-supporting medium (MesenPRO RSTM Medium, Gibco™), recommended by a manufacturer. To the cell culture medium was added L-glutamine (2 mM; Gibco™) and an antibiotic and antimycotic mixed solution (100 U/ml penicillin, 0.1 mg/ml streptomycin, and 0.25  $\mu\text{g}/\text{ml}$  amphotericin B; Gibco™). The cells were cultured at 37°C in a humidified atmosphere in the presence of 5%  $\text{CO}_2$  (New Brunswick Galaxy® 170R  $\text{CO}_2$  Incubator). Then, at 80% confluence, the cells were trypsinized and resuspended using TrypLE™ Express Enzyme without phenol red (Gibco™).

### Electromagnetic field exposure system

The EMF device consists of magnetic field applicator and a dedicated precision electric signal generator (COMEF, Poland). The cylindrical in shape magnetic field applicator (length of 24.5 cm and a diameter of 9.5/14 cm (inside/outside)) is based on low inductance coreless solenoid with the length of 19.9 cm and a diameter of 10.5 cm. The number of turns per coil is 280, the resistance of the coil is 3.6  $\Omega$  and inductance is 2.5 mH. The whole coil is within an amagnetic Teflon tube to keep it clean and sterile. This system enables to produce magnetic field frequency from 0.01 Hz to 1 kHz and magnetic flux density up to 2 mT (amplitude). The magnetic field applicator is located in the cell culture incubator (New Brunswick Galaxy® 170R CO<sub>2</sub> Incubator), where atmosphere composition temperature and humidity regulation were provided and continuously controlled.

### Low-frequency electromagnetic field exposure of adipose tissue-mesenchymal stem cells

The AT-MSCs were exposed to continuous vertically applied sinusoidal EMF with a frequency of 50 Hz and a flux density of 1.5 mT for 24, 48, and 72 h. After the third passage, AT-MSCs were plated at a density of  $9 \times 10^3$  cells/cm<sup>2</sup> in cell culture dish (22.1 cm<sup>2</sup> of growth surface area). The cells were cultured overnight at 37°C under a humidified 5% CO<sub>2</sub> environment. Then, cells were placed in the center of the homogeneous EMF area, while the control cell were grown in a separate incubator without an EMF exposure system. The incubators were maintained under identical conditions, with 5% CO<sub>2</sub> at 37°C. Treated ( $n = 3$ ) cells were conducted without additional heat generation, nor vortex motions. For the control group, cell were cultured for the same duration (24, 48, 72 h), without EMF exposure. After an appropriate time (24, 48, 72 h) cells were washed with PBS, scrubbed, and immediately taken into FTIR analyses. This experiment was carried out three times to obtain the average results and appropriate statistical value for each of the analyzed samples.

### Adipose tissue-mesenchymal stem cells morphology

After 24, 48 h, and 72 h of EMF exposure, before FTIR analyses treated cells, as well as corresponding control cells, were observed under inverted microscope (ZEISS Primovert).

### Fourier transform infrared analysis

The FTIR spectrometer, Verte  $\times 70$  v from Bruker, was used for the measurements. The advantage of the spectroscopic methods is that there is no need for the pre-processing of cells. Spectra were collected by imposition 10 ml of each sample directly on the ATR crystal and a measurement was carried out immediately (in liquid form). Each sample was examined in the mid-range of the infrared-assisted total reflection technique using a single reflection snap ATR (Attenual Total Reflectance) with diamond crystal. Data points were collected at a resolution of 2 cm<sup>-1</sup> in the range of 700–3500 cm<sup>-1</sup> of wavenumber. The background was measured as saline solution. All measurements were made in triplicates. Data collection and analysis were

performed using OPUS 7.0 Bruker Optik GmbH 2011. The spectra were normalized and baseline corrections (the concave rubberband method with 64 baseline points) were made.

### Data analysis

For all obtained spectra, baseline correction and vector normalization were applied. These operations were performed using OPUS 7.0 software (Bruker Optics Inc., Ettlingen, Germany). To obtain information about the spectra variation depending on the type of samples the PCA was performed. PCA is a nonparametric method for extracting relevant information from confusing data sets allowing to identify patterns in data and to highlight their similarities and differences. PCA reduces the dimensionality and the number of variables of the data, by maintaining as much variance as possible. Moreover, to obtain information about the similarity between the samples, hierarchical cluster analysis (HCA) was done. These two procedures were performed using Past software based on the selected spectral in fingerprint regions between 800 cm<sup>-1</sup> and 1800 cm<sup>-1</sup>. Further data analysis was performed using Wire 3.4 software.

## RESULTS AND DISCUSSION

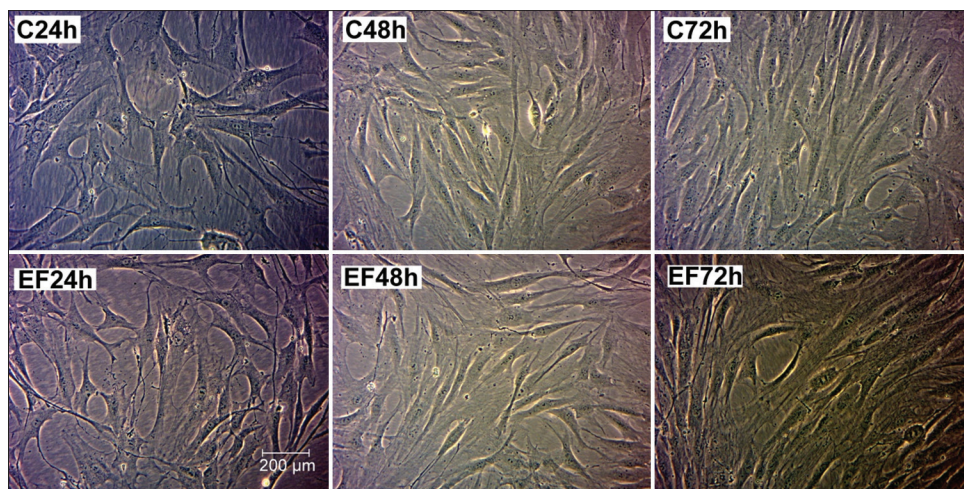
### Adipose tissue-mesenchymal stem cell morphology

Figure 1 shows the morphology of human adipose tissue-derived mesenchymal stem cells. A phase-contrast microscope ZEISS Primovert inverted microscope was used for the analysis, phase  $\times 20$  was used. The phase-contrast images of cells cultured with and without (control) exposure to the EMF are shown at three selected times (24 h, 48 h, and 72 h). It can be seen that the cells at the morphological level did not show any visible changes under the influence of EMF. The cells have the correct fusiform shape and the same size.

### Analysis of the infrared spectra of adipose tissue-mesenchymal stem cells

The FTIR absorption spectra of cells incubated with and without EMF, during 24 h (EF24 h and control-C24 h), 48 h (EF48 h and control-C48 h), and 72 h (EF72 h and control-C72 h) are reported in Figure 2. As can be seen, the spectra are highly complex, rich in many spectral lines characteristic for specific molecules building the cells. In Table 1 the positions of the observed lines and bands as well as their identification are presented.<sup>[12,30-35]</sup> This indicates the presence of changes in the cells at the molecular level, caused by the action of the EMF.

The registered spectra possess some interesting differences in their shape, as well as positions and intensity of the spectral bands. The analysis of the IR spectra of cells treated and not treated by EMFs indicates that the current changes are caused by the action of the EMF as an external environmental factor. This is visible for cells exposed to the EMF for 24 and 48 h [Figure 2a and b], comparing them to control cells (cultured for 24 and 48 h, respectively). The observed effect of the EMF on AT-MSC cells, identified by IR spectra analysis, will be discussed in detail in the next parts of this article.



**Figure 1:** Morphology of adipose tissue-mesenchymal stem cell in 3 different electromagnetic field continuous exposure durations: 24 h, 48 h, 72 h and adipose tissue-mesenchymal stem cell control ©: 24 h, 48 h, 72 h

In contrast, the spectra of cells treated with the EMF for 72 h [Figure 2c] are consistent with the recorded control spectra (cells untreated EMF). This result may indicate that the EMF causes visible changes in the cells in the first 48 h of interaction, and later homeostasis mechanisms restore the original state in terms of biochemical composition. Probably, this result may indicate the possibility of adapting the cells to the prevailing environmental conditions and regaining proper functioning after adapting to the presence of the acting factor, such as studied EMF (frequency 50 Hz). After the time when changes in cells functioning occurred at the molecular level, it may appear the adaptation to the prevailing conditions.

It should be noted that the spectrum of control cells under different incubation times (from 24 h to 72 h) also has some differences in the intensity of some IR bands or their position. This indicates the possibility of some biochemical changes occurring during cell culture associated only with the culture duration. This might seem obvious because cells during culture are dividing, becoming senescent, undergoing steps of the cell cycle. Therefore micromolecular changes might be captured. Importantly, spectra of EMF exposed samples have been adjusted to the baseline of control spectra.

The differences occurring in the IR spectra of cells treated with electromagnetic waves in comparison with control cells concern the presence of the spectral bands, their shifts, and changes in their shape. The changes occur in the region of nucleic acids ( $800\text{--}1200\text{ cm}^{-1}$ ), proteins ( $1500\text{--}1700\text{ cm}^{-1}$ ), and lipids ( $2800\text{--}3000\text{ cm}^{-1}$ ).<sup>[12,34,36]</sup> An unambiguous assessment of the occurring changes in the spectrum is not possible, it may indicate a modification of cell function at different levels (both at the stage of gene expression and protein synthesis) or the changes may also be potentially due to the impact of waves on the previously present proteins. In addition, a change in the lipid composition may indicate modification at the level of the cell membrane. A significant increase in the intensity of the

bands at  $2967\text{ cm}^{-1}$  and at  $2974\text{ cm}^{-1}$ , corresponding to the  $\text{CH}_3$  antisymmetric stretching vibration of EF24H and EF48H cells respectively, indicates an increase in the amount of saturated lipids.<sup>[31,37]</sup>

Figure 3 shows the spectra in the range of bands corresponding mainly to nucleic acids [Figure 3a] and proteins [Figure 3b]. For the first of mentioned spectral range, the changes in the IR bands composition is evident for the EF24H and EF48H sample compared to C24H and C48H, respectively. In the EF24H and EF48H spectra, the strong bands at  $1076\text{ cm}^{-1}$  and  $1071\text{ cm}^{-1}$  are assigned to the  $\text{PO}_2^-$  stretching vibration. In the C24H and C48H spectra the lines corresponding to  $\nu_s(\text{PO}_2^-)$  are localized at  $1100\text{ cm}^{-1}$  and  $1092\text{ cm}^{-1}$ . The vibrations of C-C and C-O bonds in deoxyribose also change, and they are clearly visible in the EF24H and EF48H spectra. The shift (for EF24H) and the disappearance (for EF48H) of the bands at about  $924\text{ cm}^{-1}$  and  $996\text{ cm}^{-1}$  indicate the presence of changes on the level of DNA and RNA synthesis, respectively or on the effect of EMF on previously formed nucleic acids.<sup>[38]</sup>

We noticed that at 24 and 48 h of EMF exposure the changes in nucleic acids, what may suggest that downstream signal transduction pathways might be initiated. Always after this new or more proteins are produced.

In the considered spectral region, the C-O and C-O-H vibrations of glycerol also occurs.<sup>[12,39]</sup> This line is observed in the spectrum of C24H ( $1027\text{ cm}^{-1}$ ) and C48H ( $1036\text{ cm}^{-1}$ ), while it is not clearly visible in the spectrum of cells treated with an EMF, which indicates a lower content of glycogen in cells. In the case of protein region analysis, the differences relate mainly to shifts in the position of the maximum of the recorded amide bands. More significant differences occur in the region from  $1350\text{ cm}^{-1}$  to  $1500\text{ cm}^{-1}$  where the spectral bands corresponding to proteins, lipids, and polysaccharides overlap. A detailed analysis of the amide band giving the information about the secondary structure of the cell proteins

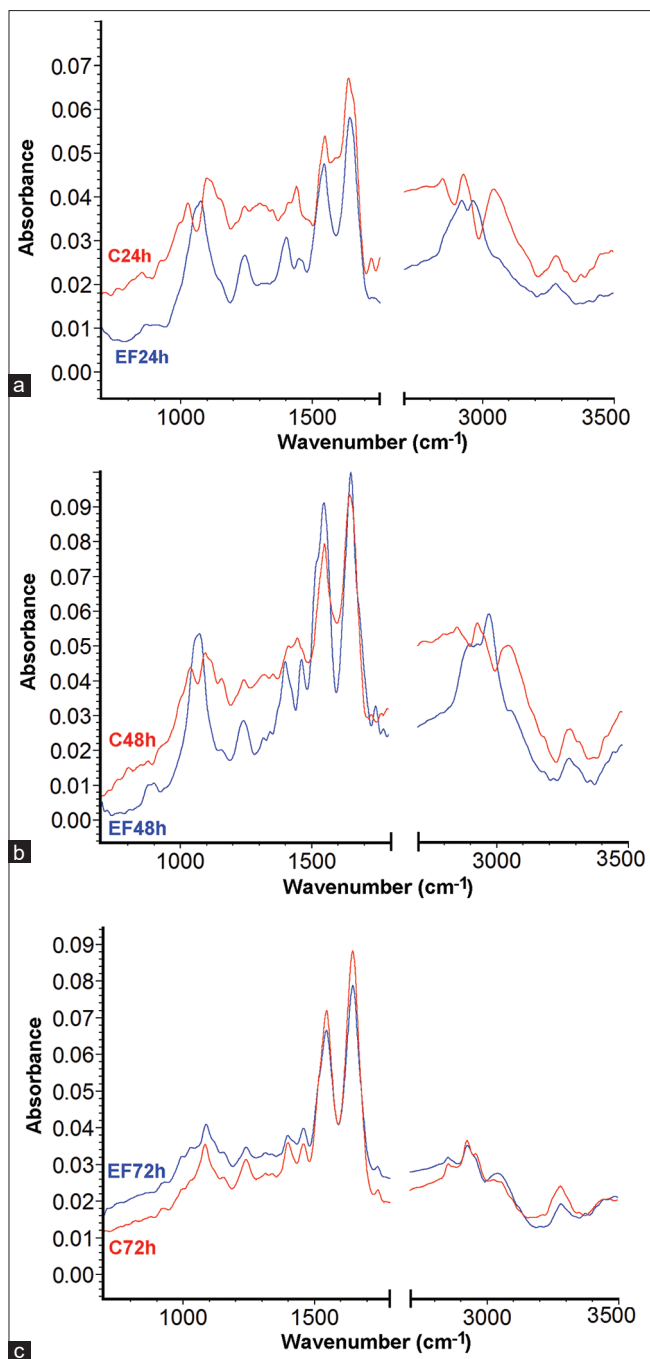


**Figure 2:** Fourier transform infrared spectra of adipose tissue-mesenchymal stem cell in electromagnetic field continuous exposure durations: (a) EF24 h and control-C24 h. (b) EF48 h and control-C48 h. (c) EF72 h and control-C72 h. Measuring range 800–3500  $\text{cm}^{-1}$

is presented below. We observed changes on protein level and conformation, as well as on lipid level.

To protein secondary structure analysis, the second derivative in the narrow spectral region of amide I band was applied. This mathematical procedure allows to resolve the bands made by several overlapping lines, whose positions cannot be easily identified.<sup>[38]</sup> The lines forming the amide I band are highly sensitive to variation in molecular geometry and

hydrogen bonding.<sup>[30]</sup> Figure 4 shows the normalized spectrum for the spectral region from 1600  $\text{cm}^{-1}$  to 1700  $\text{cm}^{-1}$  and the second derivative of the spectral lines. This allows to perform approximation of observed spectrum by Lorentzian and Gaussian functions [Figure 5]. The obtained peaks positions are collected in Table 2.

The lines located in the spectral range of 1648–1663  $\text{cm}^{-1}$  are associated with the  $\alpha$ -helical protein structure,<sup>[30,32,38,39]</sup> and their relative area provides a share of this type of structure in the examined material. The percentage of the  $\beta$ -sheets is calculated by the relative area of line occurring in the region of 1621–1638  $\text{cm}^{-1}$ .<sup>[30,32,39,40]</sup> The  $\alpha$ -helix and  $\beta$ -sheet are the most common type of protein secondary structures. Other types of the spatial structure of proteins are also registered. One of them is the  $\beta$ -turn structure which is a type of nonregular secondary structure. This structure is associated with the lines registered from 1668  $\text{cm}^{-1}$  to 1688  $\text{cm}^{-1}$ .<sup>[30,32,39,40]</sup> The band at 1642/1643  $\text{cm}^{-1}$  should be assigned to the random coil which is irregular protein structure.<sup>[30,40]</sup> The bands originating from the amino acid side chains vibrations–  $\nu(\text{C}=\text{O})$ ,  $\nu(\text{CN}_3\text{H}_5^+)$ ,  $\nu(\text{C}=\text{C})$  and  $\delta\text{NH}_2$  bands– are observed also (at about 1615  $\text{cm}^{-1}$ ).<sup>[31,32,40]</sup> In Table 2, the location of individual peaks corresponding to the structure of the protein is shown.

It should be noted, that both, change in the position of the bands and the differences of particular conformations percentage are recorded for samples under and without the influence of EMF in 24 h and 48 h incubation. As it is shown in Figure 5 and Table 2 the significant differences in spectral lines curve fitting are visible to the C24 h and EF24 h as well as C48 h and EF48 h samples. For C72 h and EF72 h samples, the differences are minimal as in the case of the other spectral regions described above. These results confirm the fact that the EMF changes the chemical composition of the AT-MSCs during the first 48 h.

Additionally, we observed, some small changes during cell culture (in 24 h, 48 h, and 72 h) without EMF exposure. This seems obvious because cells are dividing, becoming senescent, undergoing cell cycle, etc. Therefore, micromolecular changes might be captured. Importantly, spectra of EMF exposed samples have been adjusted to the baseline of control spectra.

For the C24 h cells, the clearly dominant bands that appear in the analyzed spectra corresponds to basic forms of protein conformation:  $\alpha$ -helix and  $\beta$ -sheet. In the case of EF24 h, C48 h, EF48 h, EF72 h, and C72 h cells, the bands assigned to the random coil and  $\beta$ -turn conformation, as well as amino acids side chains vibrations are observed. This is important information because it indicates that the EMF changes the structure of proteins in the cells after 24 h. While the same spontaneous changes occur in control only after 48 h and 72 h.

As mentioned previously, the detailed analysis of amide I band gave the information on the secondary structure of the cell proteins.<sup>[37]</sup> The concentration of the main protein conformation ( $\alpha$ -helix,  $\beta$ -sheet and other) for each investigated

Table 1: Vibrational frequencies and assignments of infrared peaks found in the stem cells spectra

Control 24h (c24h) (cm <sup>-1</sup> )	Electro-magnetic field 24h (ef24h) (cm <sup>-1</sup> )	Control 48h (c48h) (cm <sup>-1</sup> )	Electro-magnetic field 48h (EF48H) (cm <sup>-1</sup> )	Control 72h (C72h) (cm <sup>-1</sup> )	Electro-magnetic field 72h (EF72h) (cm <sup>-1</sup> )	Vibrations	Assignment
852	-	847	-	-	-	$\gamma$ (O-H)	
-	864	-	877	-	-	C-C, C-O deoxyribose	DNA
924	917	924	-	923	924	Left hand helix DNA (Z form)	DNA
993sh	990 sh	996 sh	-	996 sh	994sh	$\nu$ (P-O-C), $\nu$ (C-O) ribose, C-C	RNA, DNA
1027	-	1036	-	-	1030	C-O, C-O-H	Glycogen
-	1076	-	1071	-	-	$\nu_s$ (PO <sub>2</sub> )	DNA
-	-	-	-	1084	1088	$\nu_s$ (PO <sub>2</sub> ), P-O-C	
1100	-	1092	-	-	-	$\nu_s$ (PO <sub>2</sub> ), P-O-C	
1153	1151 sh	1155	1155	1153	1153	$\nu$ (C-O), $\nu$ (C-C), def. C-O-H	RNA, DNA Proteins, glycogen, carbohydrates
1243	1243	1240	1239	1240	1240	Amide III ( $\nu$ (CN), $\delta$ (NH), $\delta$ (CO), $\nu$ (CC)), $\nu_{as}$ (PO <sub>2</sub> )	Proteins, DNA, phospholipids
1302	1308	1316	1315	1314	1315	Amide III ( $\nu$ (CN), $\delta$ (NH), $\delta$ (CO), $\nu$ (CC)) and def. N-H	Proteins
1349	1328	1351	1341	1339	1338	$\omega$ (CH <sub>2</sub> )	Proteins, lipids, polysaccharides
1411	1403	1410	1398	1410	1399	$\nu$ (C-N), def. N-H, def. C-H	Proteins
1441	1450	1444	1460	1459	1459	def. CH <sub>2</sub> , def. C-H	Lipids, fatty acids, proteins, polysaccharides
1549	1547	1548	1545	1547	1547	Amide II ( $\delta$ (NH), $\nu$ (CN), $\delta$ (CO), CC, $\nu$ (NC))	Proteins
1639	1644	1644	1648	1646	1647	Amide I ( $\nu$ (C=O), $\nu$ (CN), $\gamma$ (CCN), $\delta$ (NH))	Proteins
1726	1734	1726	1741	1741	-	$\nu_{as}$ (C=O)	Lipids, fatty acids esters, RNA, DNA
1762	-----	-----	1742	1741	1741	$\nu$ (C=C)	Lipids fatty acids
2850	-----	2853	-----	2854	2853	$\nu_s$ (CH <sub>2</sub> )	Lipids, proteins
2929	2924	2930	2931	2926	2927	$\nu_{as}$ (CH <sub>2</sub> )	Lipids, proteins
-----	2967	-----	2974	-----	-----	$\nu_{as}$ (CH <sub>3</sub> )	Lipids, proteins
3044	-----	3047	3053	3025	3043	$\nu$ (N-H) (amide B)	Proteins
3283	3281	3281	3279	3283	3283	$\nu$ (N-H) (amide A), $\nu$ (O-H)	Proteins, O-H stretching (water)

Sh: Shoulder,  $\nu$ : Stretching vibration,  $\nu_s$ : Symmetric stretching vibration,  $\nu_{as}$ : Antisymmetric stretching vibration,  $\delta$ : Deformation in plane bending vibration,  $\gamma$ : Deformation out of plane vibration

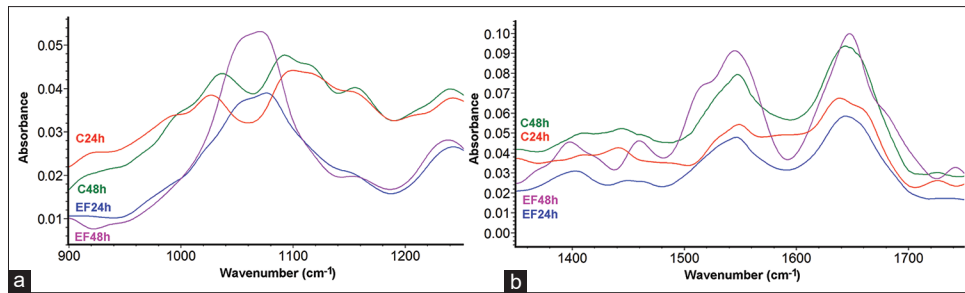


**Figure 3:** Fourier transform infrared spectrum of the peaks derived from nucleic acids (a) and proteins (b) of adipose tissue-mesenchymal stem cell in 2 different electromagnetic field continuous exposure durations: EF24 h, EF48 h and adipose tissue-mesenchymal stem cell control: C24 h, C48 h. Measuring range 900–1225 cm<sup>-1</sup>

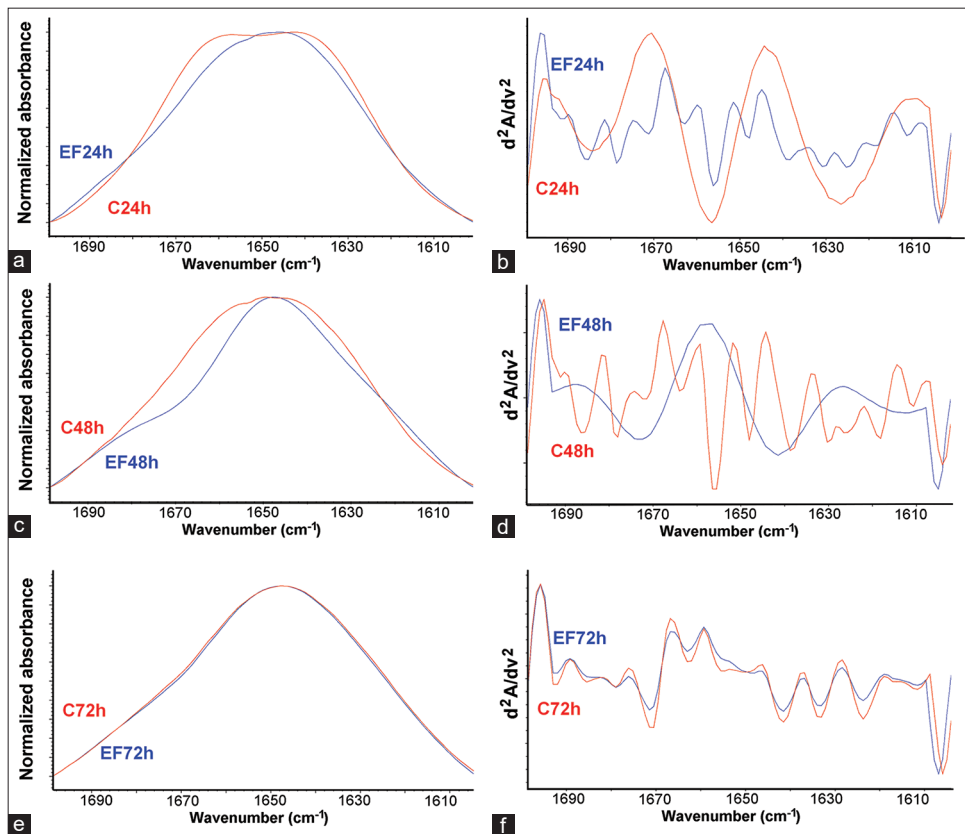


**Figure 4:** Normalized Fourier transform infrared spectra and second derivative spectra of EF24 h and control-C24 h (a and b), EF48 h and control-C48 h (c and d) EF72 h and control-C72 h (e and f) in the 1600–1700 cm<sup>-1</sup> region

sample are presented in Figure 6 and Table 3. The relative participation of these components seemed to change, which indicates differences in the protein expression or action of EMF on pre-existing proteins by changing their structure. However, in the case of the cells under the influence of the EMF for the longest time (72 h), these changes between C72 h and EF72 h samples are minimal (1%–2%). The  $\alpha$ -helix structure is dominant in all types of tested samples. The presence of this conformation varies from about 65% (for the cells incubated during 24 h without exposure to electromagnetic radiation) to 30% (for the cells incubated during 24 h with exposure to electromagnetic radiation). Natural changes in culture over

time and the effects of EMF cause a change in the structure of proteins by destroying the alpha helix. For the EF48 h, C48 h, EF72 h, and C72 h the  $\alpha$ -helix participation was 47%, 44%, 39%, 38%. Significant changes can also be seen with the  $\beta$ -sheet structure for EF24 h, C24 h, EF48 h, C48 h cells and amounted 24%, 35%, 45%, and 35%, respectively. For the cells incubated during 72 h it was about 30%–31%. Obtained results may indicate a change in protein expression, reduction in synthesis of helix-like proteins (alpha-myosin for example<sup>[37]</sup>) and  $\beta$  sheet-like proteins and increasing a turns-like and irregular proteins, due to the EMF influence for 24 h.

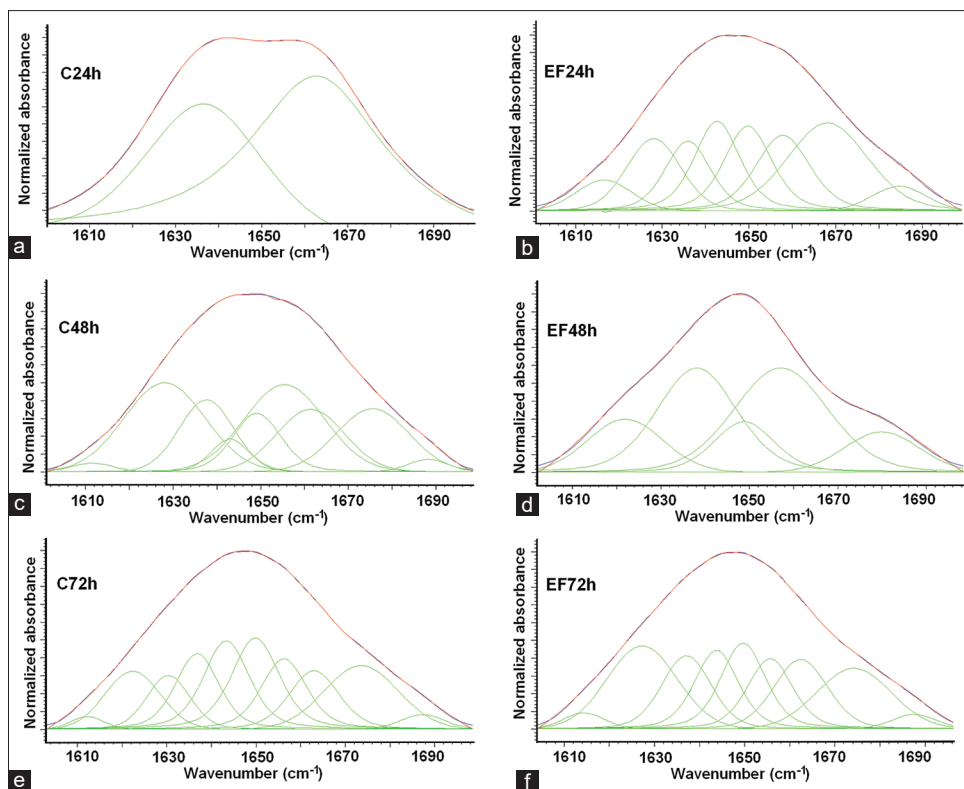


**Figure 5:** Curve-fitting of the amide I band of C24 h (a), EF24 h (b), C48 h (c) EF48 h (d), C72 h (e), and EF72 h (f) in the 1600–1700 cm<sup>-1</sup> region

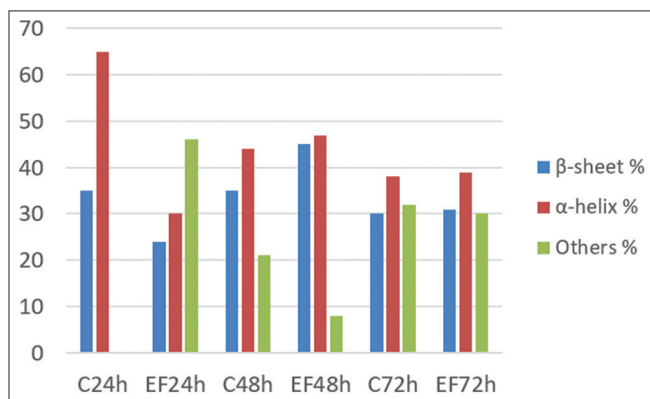


**Figure 6:** Protein secondary structure composition (%) of C24 h, EF24 h, C48 h, EF48 h, C72 h and EF72 h

**Table 2: Assignment of amide I band position to secondary structure**<sup>[30,32,38,39]</sup>

Protein secondary structure	Time 24 h		Time 48 h		Time 72h	
	EF24h	C24h	EF48h	C48h	EF72h	C72h
Side chain	1616	-	-	1611	1614	1612
β-sheet	-	-	1621	-	-	1622
β-sheet	1628	-	-	1628	1627	1630
β-sheet	1636	1636	1638	1637	1637	1636
Random	1642	-	-	1643	1643	1643
α-helix	1649	-	1648	1649	1650	1650
α-helix	1658	-	1657	1655	1655	1656
α-helix	-	1663	-	1661	1662	1663
β-turn	1668	-	-	1675	1674	1673
β-turn	1685	-	1680	1688	1687	1687

### Multivariate principal component analysis and hierarchical cluster analysis

PCA Figure 7a showed FTIR spectra obtained from samples of AT-MSC. Regarding component 1, two groups are formed, the first of which contains ATMSCs samples in the EMF incubated for 24 h and 48 h, what means that they are similar to each other. In contrast, the second group are samples from controls (24 h and 48 h), what also suggests strong similarities between these samples. PCA analysis shows that there is a significantly different biochemical composition between Group I and Group II, which confirms the strong effect of EMF on the treated cells.

In the case of the 72 h control sample, it is closer to the EMF 24 h and EMF 48 h samples, but located more on the border of both groups which indicates the existence of other biochemical variables in it. In contrast, the EMF 72 h sample is in the group with controls, and this means that after 72 h there was no strong effect of the EMF on the biochemical composition of the cells.

These observations from PCA analysis is confirmed by an HCA [Figure 7b]. The dendrogram of HCA created two initial clusters presented by two branches, and the first of them were further subdivided into smaller clusters. As shown in Figure 7b, the AT-MSC samples of all control and EMF



**Table 3: Protein secondary structure composition (%), according to relative area of component bands**

	$\beta$ -sheet (%)	$\alpha$ -helix (%)	Others (%)
EF24h	24	30	46
C24h	35	65	-
EF48h	45	47	8
C48h	35	44	21
EF72h	31	39	30
C72h	30	38	32

in 72 h were classified as cluster I, which means that the biochemical composition in these samples is similar. Moreover, it was divided into two additional clusters that points to strong similarities between samples C24 h and C48 h the same as between C72 h and EF72 h. Clusters II include samples of AT-MSC in EF48 h and EF24 h that showed similarities between these two groups, indicating similar biochemical variables in these samples.

Both analyzes: PCA and HCA showed that the largest differences occurred at 24 and 48 h of EMF exposure, which means that during the first 48 h, EMF affects proteins, fats, and nucleic acids by changing their structure.

## CONCLUSIONS

Cells/Stem cells respond to external factors coming from their environment/stem cell niche. Cells were co-evolving together with the natural EMF. However to artificial EMF we are currently being adapting, and so the stem cells in *in vitro* culture.

The first response of cells is on the micromolecular level, which is not even visible in functional or morphological levels, sometimes not even in protein or gene expression levels. During this very dynamic molecular stage, many processes including those reversible, have taken place. FTIR gives the possibility to monitor early subtle changes, which may manifest later during the process of adaptation, or when stem cells changes its status. These afterward changes can be seen on the epigenome, transcriptome, proteome level, and so on. From currently available literature, we know that EMF strongly influences many internal mesenchymal stem cell processes such as proliferation, viability, cell cycle, carcinogenesis, differentiation, and death.

FTIR spectra show differences between samples under the influence of EMF before they will be manifested at the morphological level. Presented analyzes support our supposition that EMFs affect adipose tissue-derived mesenchymal stem cells. The largest differences in the range of nucleic acids and proteins in the fingerprint region occurred at 24 and 48 h of EMF exposure. That means that during the first 48 h, when a great number of dynamic changes occurred, EMF affects micromolecular composition of proteins, fats, and nucleic acids and therefore changes their structure. However, in the case of AT-MSCs in 72 h EMF and 72 h control, no

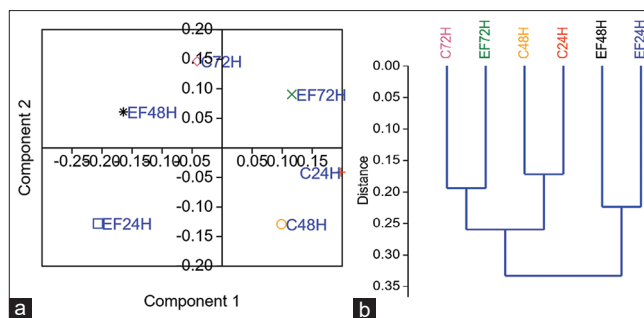


**Figure 7:** Principal component analysis (a) and hierarchical cluster analysis (b) analysis of adipose tissue-mesenchymal stem cell control in 3 different times and adipose tissue-mesenchymal stem cell in 3 different electromagnetic field continuous exposure durations obtained from attenuated total reflection-Fourier transform infrared spectroscopy. Two-dimensional scores plot of samples with differences in chemical compositions presented in the fingerprint region

significant differences were noted in the FTIR spectra, which means that the chemical composition in these two cases is similar. EMF is not neutral for stem cells, especially in the in the first hours of interaction (24 h, 48 h).

This led us to the conclusion that we should analyze very early stages of EMF exposure and monitor the changes at each and every hour until 48 h. It is very interesting that even if we do not see any changes at the morphological level, it does not mean nothing happens within the cells.

Our results are promising and justify conducting further research on the use of FTIR and future FTIR technologies for diagnosis, monitoring of differentiation, and determination of the neoplastic status of human adipose tissue-derived mesenchymal stem cells.

## HIGHLIGHTS

1. Effect of low-frequency EMF on mesenchymal stem cells derived from adipose tissue
2. AT-MSC at 3 different continuous EMF exposure times: 24 h, 48 h, 72 h
3. Searching for differences in spectra obtained using FTIR spectroscopy
4. Presentation of the changes in the spectra of proteins and nucleic acids between samples.

## Financial support and sponsorship

Nil.

## Conflicts of interest

There are no conflicts of interest.

## REFERENCES

1. Pittenger MF, Mackay AM, Beck SC, Jaiswal RK, Douglas R, Mosca JD, *et al.* Multilineage potential of adult human mesenchymal stem cells. *Science* 1999;284:143-7.
2. Yan J, Dong L, Zhang B, Qi N. Effects of extremely low-frequency magnetic field on growth and differentiation of human mesenchymal stem cells. *Electromagn Biol Med* 2010;29:165-76.

3. Banas A, Teratani T, Yamamoto Y, Tokuhara M, Takeshita F, Osaki M, *et al.* IFATS collection: *In vivo* therapeutic potential of human adipose tissue mesenchymal stem cells after transplantation into mice with liver injury. *Stem Cells* 2008;26:2705-12.
4. Moody B, Haslauer CM, Kirk E, Kannan A, Lobo EG, McCarty GS. *In situ* monitoring of adipogenesis with human-adipose-derived stem cells using surface-enhanced Raman spectroscopy. *Appl Spectrosc* 2010;64:1227-33.
5. Kocan B, Maziarz A, Tabarkiewicz J, Ochiya T, Banaś-Ząbczyk A. Trophic activity and phenotype of adipose tissue-derived mesenchymal stem cells as a background of their regenerative potential. *Stem Cells Int* 2017;2017:1653254.
6. Belyaev I, Dean A, Eger H, Hubmann G, Jandrisovits R, Kern M, *et al.* EUROPAEM EMF Guideline 2016 for the prevention, diagnosis and treatment of EMF-related health problems and illnesses. *Rev Environ Health* 2016;31:363-97.
7. IARC Working Group on the Evaluation of Carcinogenic Risks to Humans 2002 Non-ionizing radiation, Part I: Static and extremely low-frequency (ELF) electric and magnetic fields. *IARC Monogr Eval Carcinog Risks Hum* 2002;80:1-395.
8. IARC Working Group on the Evaluation of Carcinogenic Risks to Humans 2011 Non-ionizing radiation, Part II: Radiofrequency electromagnetic fields. *IARC Monogr Eval Carcinog Risks Hum* 2011;102:407-19.
9. Maziarz A, Kocan B, Bester M, Budzik S, Cholewa M, Ochiya T, *et al.* How electromagnetic fields can influence adult stem cells: Positive and negative impacts. *Stem Cell Res Ther* 2016;7:54.
10. Jimenez H, Blackman C, Lesser G, Debinski W, Chan M, Sharma S, *et al.* Use of non-ionizing electromagnetic fields for the treatment of cancer. *Front Biosci (Landmark Ed)* 2018;23:284-97.
11. Hoffman LM, Carpenter MK. Characterization and culture of human embryonic stem cells. *Nat Biotechnol* 2005;23:699-708.
12. Movasaghi Z, Rehman S, Rehman I. Fourier transform infrared (FTIR) spectroscopy of biological tissues. *Appl Spectrosc Rev* 2008;43:134-79.
13. Vazquez-Zapian GJ, Mata-Miranda MM, Sanchez-Monroy V, Delgado-Macuul RJ, Perez-Ishiwara DG, Rojas-Lopez M. FTIR spectroscopic and molecular analysis during differentiation of pluripotent stem cells to pancreatic cells. *Stem Cells Int* 2016;2016:6709714.
14. Aksoy C, Severcan F. Role of vibrational spectroscopy in stem cell research. *J Spectrosc* 2012;27:167-84.
15. Cao J, Ng ES, McNaughton D, Stanley EG, Elefanti AG, Tobin MJ, *et al.* The characterisation of pluripotent and multipotent stem cells using Fourier transform infrared microspectroscopy. *Int J Mol Sci* 2013;14:17453-76.
16. Larkin PJ. *Infrared and Raman Spectroscopy: Principles and Spectral Interpretation*. San Diego, CA, USA: Elsevier; 2011.
17. Mourant JR, Gibson RR, Johnson TM, Carpenter S, Short KW, Yamada YR, *et al.* Methods for measuring the infrared spectra of biological cells. *Phys Med Biol* 2003;48:243-57.
18. Boydston-White S, Gopen T, Houser S, Bargonetti J, Diem M. Infrared spectroscopy of human tissue. V. Infrared spectroscopic studies of myeloid leukemia (ML-1) cells at different phases of the cell cycle. *Biospectroscopy* 1999;5:219-27.
19. Cohenford MA, Rigas B. Cytologically normal cells from neoplastic cervical samples display extensive structural abnormalities on IR spectroscopy: Implications for tumor biology. *Proc Natl Acad Sci U S A* 1998;95:15327-32.
20. Pevsner A, Diem M. Infrared spectroscopic studies of major cellular components. Part I: The effect of hydration on the spectra of proteins. *Appl Spectrosc* 2001;55:788-93.
21. Pevsner A, Diem M. Infrared spectroscopic studies of major cellular components. Part II: The effect of hydration on the spectra of nucleic acids. *Appl Spectrosc* 2001;55:1502-5.
22. Jackson M, Mantsch HH. The use and misuse of FTIR spectroscopy in the determination of protein structure. *Crit Rev Biochem Mol Biol* 1995;30:95-120.
23. Hocdé S, Boussard-Plédel C, Fonteneau G, Lucas J. Chalcogens based glasses for IR fiber chemical sensors. *Solid State Sci* 2001;3:279-84.
24. Goormaghtigh E, Raussens V, Ruyschaert JM. Attenuated total reflection infrared spectroscopy of proteins and lipids in biological membranes. *Biochim Biophys Acta* 1999;1422:105-85.
25. Minnes R, Nissinmann M, Maizels Y, Gerlitz G, Katzir A, Raichlin Y. Using Attenuated Total Reflection-Fourier Transform Infra-Red (ATR-FTIR) spectroscopy to distinguish between melanoma cells with a different metastatic potential. *Sci Rep* 2017;7:4381.
26. Razavi S, Salimi M, Shahbazi-Gahreuei D, Karbasi S, Kermani S. Extremely low-frequency electromagnetic field influences the survival and proliferation effect of human adipose derived stem cells. *Adv Biomed Res* 2014;3:25.
27. Ross CL. The use of electric, magnetic, and electromagnetic field for directed cell migration and adhesion in regenerative medicine. *Biotechnol Prog* 2017;33:5-16.
28. Todorova N, Bentvelzen A, English NJ, Yarovsky I. Electromagnetic-field effects on structure and dynamics of amyloidogenic peptides. *J Chem Phys* 2016;144:085101.
29. Mourant JR, Yamada YR, Carpenter S, Dominique LR, Freyer JP. FTIR spectroscopy demonstrates biochemical differences in mammalian cell cultures at different growth stages. *Biophys J* 2003;85:1938-47.
30. Kong J, Yu S. Fourier transform infrared spectroscopic analysis of protein secondary structures. *Acta Biochim Biophys Sin (Shanghai)* 2007;39:549-59.
31. Coates J. Interpretation of infrared spectra, a practical approach. In: Meyers RA, editor. *Encyclopedia of Analytical Chemistry*. Chichester: John Wiley and Sons Ltd.; 2006.
32. Barth A. Infrared spectroscopy of proteins. *Biochim Biophys Acta* 2007;1767:1073-101.
33. Barth A. The infrared absorption of amino acid side chains. *Prog Biophys Mol Bio* 2000;74:141-73.
34. Talari AC, Martinez MA, Movasaghi Z, Rehman S, Rehman IU. Advances in Fourier transform infrared (FTIR) spectroscopy of biological tissues. *Appl Spectrosc Rev* 2017;52:456-506.
35. Chaber R, Lach K, Szmuc K, Michalak E, Raciborska A, Mazur D, *et al.* Application of infrared spectroscopy in the identification of Ewing sarcoma: A preliminary report. *Infrared Phys Technol* 2017;83:200-5.
36. Baker MJ, Trevisan J, Bassan P, Bhargava R, Butler HJ, Dorling KM, *et al.* Using Fourier transform IR spectroscopy to analyze biological materials. *Nat Protoc* 2014;9:1771-91.
37. Stuart BH. *Infrared Spectroscopy. Fundamentals and Application*. Chichester: John Wiley and Sons; 2004.
38. Ami D, Neri T, Natalello A, Mereghetti P, Doglia SM, Zanoni M, *et al.* Embryonic stem cell differentiation studied by FT-IR spectroscopy. *Biochim Biophys Acta* 2008;1783:98-106.
39. Mobili P, Londero A, Maria TM, Eusebio ME, De Antoni GL, Fausto R, *et al.* Characterization of S-layer proteins of *Lactobacillus* by FTIR spectroscopy and differential scanning calorimetry. *Vib Spectrosc* 2009;50:68-77.
40. Delfino I, Portaccio M, Della Ventura B, Mita DG, Lepore M. Enzyme distribution and secondary structure of sol-gel immobilized glucose oxidase by micro-attenuated total reflection FT-IR spectroscopy. *Mater Sci Eng C* 2013;33:304-10.